Discerning Membrane Steady-State Oxygen Flux by Monte Carlo Markov Chain Modeling

22

Gary Angles and Sally C. Pias

Abstract

Molecular oxygen (O_2) permeability coefficients for lipid bilayers have previously been estimated using both electron paramagnetic resonance (EPR) oximetry and molecular dynamics simulation data. Yet, neither technique captures the fluxes that exist physiologically. Here, the dynamic steady state is modeled using a stochastic approach built on atomic resolution molecular dynamics simulation data. A Monte Carlo Markov chain technique is used to examine membrane-level fluxes of oxygen in lipid-water systems. At steady state, the concentration of oxygen is found to be higher inside the model membranes than in surrounding water, consistent with the known favorable partitioning of O_2 toward the lipid phase. Pure phospholipid 1-palmitoyl,2-oleoyl-phosphatidylcholine (POPC) bilayers accrue ~40% more O_2 molecules at steady state than POPC/cholesterol bilayers (1:1 molecular ratio) mimicking the red blood cell membrane. Steady-state levels of oxygen were reached inside both bilayer types within the same timeframe, but depletion of oxygen from the bilayer interior occurred 17% faster for POPC than for POPC/cholesterol. Likewise, first-order rate constants estimated for accrual to steady state were the same for POPC and POPC/cholesterol, at 190 μs⁻¹, while first-order rate constants for depletion of the accrued O_2 from the bilayers differed, at 95 μs⁻¹ for POPC and 81 μs⁻¹ for POPC/cholesterol (lower by 15%). These results are consistent with prior experiments in red blood cells (RBCs) with varying membrane cholesterol content, in which additional cholesterol slowed oxygen uptake and release. Further work is needed to understand whether differences in RBC membrane cholesterol content would affect the delivery of oxygen to tissues.

22.1 Introduction

Poor delivery of oxygen within tissues has been implicated as a possible cause of health anomalies associated with hypoxia, which may result from high tissue oxygen demand and/or low oxygen supply [1]. Oxygen transport depends on circulating red blood cells (RBCs), which take up

G. Angles · S. C. Pias (✉)

Department of Chemistry, New Mexico Institute of Mining and Technology (New Mexico Tech), Socorro, NM, USA
e-mail: sally.pias@nmt.edu

oxygen in the alveolar capillaries through binding to hemoglobin. In tissues, O_2 release from hemoglobin generates a momentary oxygen gradient across the RBC membrane. This gradient drives O_2 transport across the membrane and involves a momentary steady state at the membrane level. Under normal physiological conditions, RBC membranes have a cholesterol-to-phospholipid molecular ratio of 1:1 or 50 mol% cholesterol [2]. Cholesterol at this level has been shown to slow the penetration of molecular oxygen [3, 4], but our previous work suggests that cholesterol-rich lipid bilayers should not be rate-limiting for oxygen diffusive transport [1].

Electron paramagnetic resonance (EPR) spin-label oximetry has provided valuable experimental data on membrane-level oxygen transport in 1-palmitoyl,2-oleoyl-phosphatidylcholine (POPC) and 1:1 POPC/cholesterol bilayers [2]. We have conducted prior molecular dynamics (MD) simulation studies of oxygen transport, which compare well with the EPR data and generate additional insight [1, 3]. In both the EPR and the MD techniques, observations are generated from systems at equilibrium, where the rate of oxygen diffusion in each direction is equal. Oxygen is neither consumed nor generated and, therefore, a steady state cannot be established. In contrast, biological oxygen transport occurs primarily under unidirectional, nonequilibrium steady-state conditions, where metabolic consumption of oxygen drives its transport.

The MD method does not readily support nonequilibrium simulations, as periodic boundary conditions are required to avoid boundary effects and to handle long-range electrostatic interactions. The use of periodic boundary conditions, where a molecule that leaves the simulation box on one side reenters on the opposite side, enables small-nanoscale systems (e.g., 30,000 atoms) to be treated as infinitely large, approximating the behavior of real macroscopic systems. While valuable for studying membrane permeation processes at atomic resolution, the MD technique alone does not provide a basis for studying steady-state flux. We have sought to overcome this limitation through stochastic modeling.

To probe unidirectional steady-state flux, we have developed a Monte Carlo Markov chain (MCMC) modeling technique [4] based on MD diffusional trajectories of O_2 molecules. The MCMC technique uses a Monte Carlo (random) simulator to propagate motion of oxygen molecules by way of a transition probability matrix built from MD simulations. The propagation of O_2 molecules across a lipid bilayer is treated as a Markov process, where the assumption is made that the probability for an O_2 molecule to transition to a new spatial position depends only on its current position. This MCMC technique enables approximation of unidirectional steady-state oxygen flux and overcomes the limitations of periodic boundary conditions while benefitting from the atomic resolution of unrestrained atomistic MD simulations.

Here, we use our MCMC technique to study the ebb and flow of oxygen at the level of a model lipid bilayer representing the RBC membrane as O_2 is taken up in the lungs or released in tissues. The MCMC technique enables generation of an oxygen gradient across a lipid bilayer, by holding the oxygen concentration on one side constant and by consuming oxygen on the other side. Due to its nonpolarity and small size, oxygen is at least three times more soluble in lipids than in water [5]. Therefore, at steady state, the oxygen content of the bilayer exceeds that of neighboring water.

We first study systems as they progress toward and then reach steady-state oxygen flux, as indicated by a constant number of O_2 molecules within the bilayer. Then, we study the depletion process for oxygen contained in a bilayer by ceasing to add O_2 molecules on the supply side and continuing to remove them on the consumption side. We compare these "accrual" and "depletion" processes for lipid bilayers composed of 1:1 POPC/cholesterol (RBC mimic) and POPC without cholesterol (control), to illuminate the role of cholesterol in RBC membrane-leveloxygen transport.

22.2 Methods

All-atom, unrestrained molecular dynamics simulations of hydrated POPC and POPC/cholesterol bilayers incorporating O_2 were used as the basis for constructing the Markov transition matrix. Conditions of the MD simulations were identical to those in our earlier work [1], with the following exceptions. First, the temperature was controlled using Langevin dynamics with a collision frequency of 1 ps^{-1}. Second, the O_2 model was adjusted to correct for overpartitioning toward the lipid phase, by adopting the Lennard-Jones parameters for the ester carbonyl oxygen (oC) atom type in the Lipid14 force field; all other O_2 model parameters were maintained as in Ref. [1]. Finally, 15–45% higher O_2 levels were used, namely, 40 O_2 molecules in the POPC simulation system or 44 O_2 in the POPC/cholesterol system, along with 128 lipids and 4440 water molecules. The results of the current work are consistent with simulations done at the lower O_2 levels (data not shown).

For each bilayer system, a transition matrix for O_2 was constructed along the lipid bilayer normal (the axis of permeation, or z axis), using bins spaced at 1 Å intervals and a time step of 1 ps. For binning, only the depth of the oxygen molecules along this z axis was considered (ignoring the xy spatial distribution, which does not contribute directly to permeation). MD trajectories for 40 or 44 O_2 molecules over 156 ns with 1 ps sampling (6–7 million data points) were pooled to generate the matrix, which held the probabilities of O_2 molecule transition from every bin to every other bin along the z axis. Thus, the number of rows and columns of the matrix was equal and matched the number of 1 Å bins required to encompass the whole system, including the lipid bilayer and surrounding water layers.

After construction of the transition matrix, Monte Carlo moves were used to generate "runs" simulating O_2 transport at 1 ps and 1 Å (in z) intervals, with spatial transitions influenced by the probabilities held in the matrix. More specifically, the instantaneous O_2 molecule configuration along the z axis was held in a Markov chain

vector, π_t. This vector was transformed by the transition probability matrix, P, resulting in a subsequent oxygen configuration, π_{t+1}. The configuration was iteratively transformed by the transition matrix to yield subsequent configurations, π_{t+2} and so on: $P\pi_t = \pi_{t+1}$, $P\pi_{t+1} = \pi_{t+2}$, etc. O_2 molecules were treated as whole particles, i.e., fractional occupation of a particular bin was disallowed. The code was developed using the Python programming language [6].

For the steady-state scheme, an oxygen concentration gradient was generated by holding the number of O_2 molecules constant on one side of the bilayer and consuming O_2 molecules on the other side. For POPC/cholesterol, the "supply" zone consisted of water layer bins 0–6 (Å), and the "consumption" zone consisted of water layer bins 88–94. For POPC, the supply zone spanned bins 0–6, and the consumption zone bins 68–73. (These zones are shaded in Fig. 22.1)

22.3 Results and Discussion

To study oxygen accrual within POPC/cholesterol and POPC lipid bilayers as each system progressed toward steady state, the total number of O_2 molecules in the system was initially set to zero. At each subsequent time step of an MCMC run, a threshold of 2 O_2 molecules was applied in the supply zone of the water region ("entry side" shaded areas in Fig. 22.1a, b), and one O_2 molecule was added at each time step if needed to meet the threshold. O_2 molecules were added in the supply zone, as needed to maintain at least two molecules in this zone at each time step. When the number of O_2 molecules accrued within the lipid bilayer reached a plateau, the system was considered to have reached steady state.

The steady-state accrual levels were 56 O_2 molecules for POPC (Fig. 22.1c) and 34 O_2 molecules for POPC/cholesterol (Fig. 22.1d). These levels reflect lower solubility of O_2 in cholesterol-rich bilayers [1]. Twenty 100 ns accrual runs (blue lines) were conducted for each bilayer system, and their running average is shown (black line). For both the POPC and the POPC/choles-
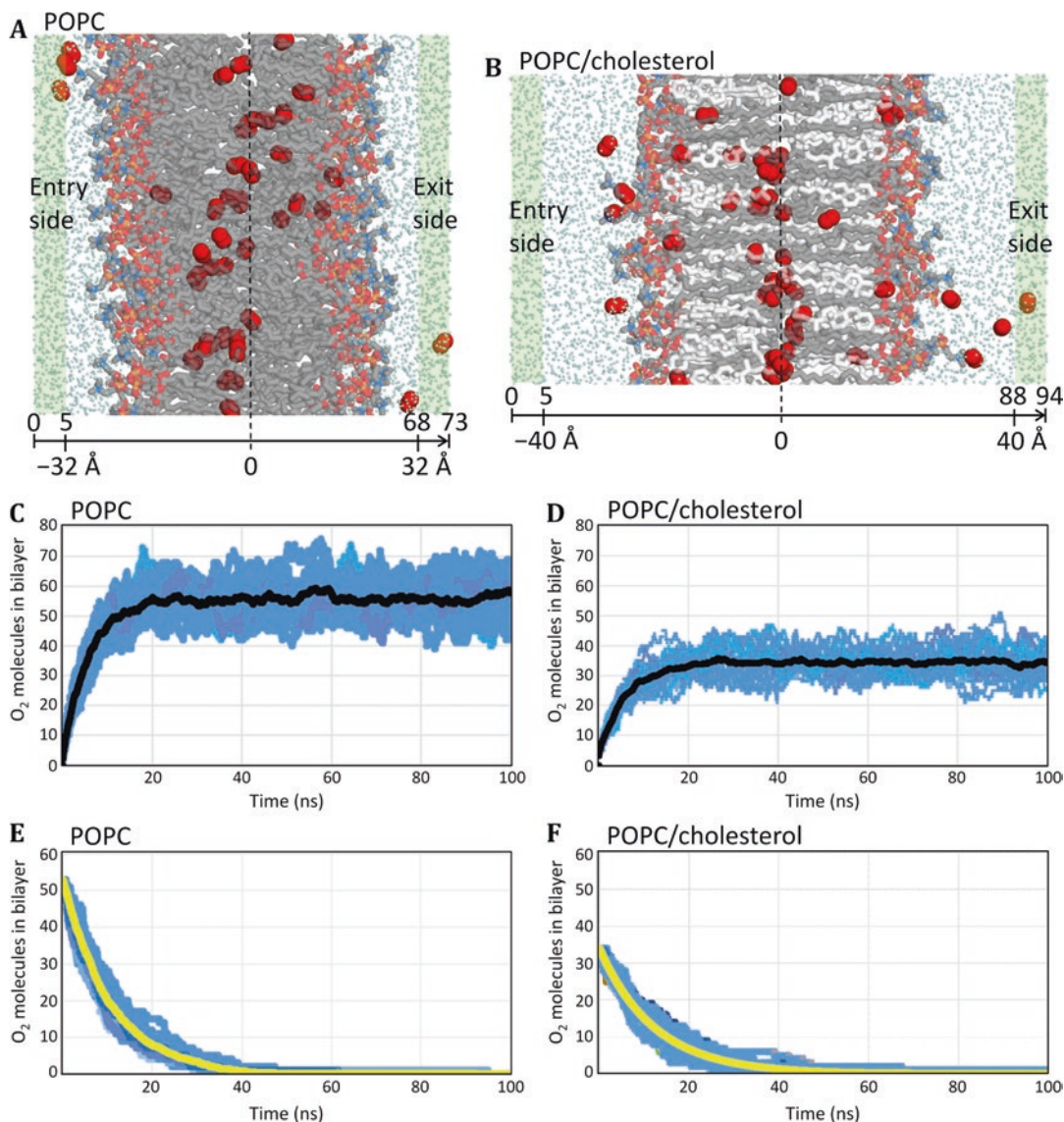
Fig. 22.1 (**a**, **b**) Schematic representations of the MCMC steady-state models for the POPC and POPC/cholesterol bilayer systems. The bilayer images are MD simulation snapshots, with O_2 shown as red spheres, POPC as gray sticks with headgroups colored by element, cholesterol as white sticks, and surrounding water molecules as reduced-size dots. All H atoms hidden for clarity. (**c**, **d**) Accrual curves showing progression to steady state in POPC and POPC/cholesterol. Black curves are the average of 20 MCMC runs (blue lines). (**e**, **f**) Depletion curves for POPC and POPC/cholesterol. Yellow curves are the average of 20 runs (blue lines)

terol bilayer systems, steady state was reached within ~24 ns.

To study depletion of oxygen from the bilayers after reaching steady state, removal of O_2 molecules in the consumption zone was continued, while no further molecules were added in the supply zone. As before, 20×100 ns runs were conducted for each bilayer system (blue lines in Fig. 22.1e, f), and their running average is shown (yellow lines). As expected, the number of O_2 molecules within each lipid bilayer diminished, rapidly at first and then more slowly. Full depletion of O_2 occurred within ~48 ns for POPC and ~56 ns for POPC/cholesterol (17% longer).

Mathematical regression of the curves revealed the rates of accrual and depletion to be first order (dependent only on the O_2 concentration). The rate constants for accrual, k_{accr}, were calculated to be 190 µs^{-1} (or 1.9×10^8 s^{-1}) for both POPC and POPC/cholesterol. The rate constants for depletion, k_{depl}, reflect the differences in the depletion curves and are estimated to be 95 µs^{-1} (or 9.5×10^7 s^{-1}) for POPC and 81 µs^{-1} for POPC/cholesterol (lower by 15%). This difference is consistent with the ~10% reduction of 50 mol% POPC/cholesterol permeability relative to POPC estimated in our previous work, based on equilibrium MD simulations [1]. The kinetics observed here are also congruent with experimental work by Buchwald and colleagues, in which both the kinetics and the amount of O_2 uptake and release by RBCs were found to diminish with above-normal RBC membrane cholesterol content [7].

22.4 Conclusions and Expansion of the Model

The steady-state stochastic MCMC technique piloted here shows promise to generate valuable insights into physiological oxygen transport by RBCs. It also provides a basis for interpreting other experimental findings, such as magnified O_2 gradients across cholesterol-enriched Chinese hamster ovary (CHO) cell plasma membranes observed by Swartz and colleagues [8]. Moreover, the MCMC technique enables rapid simulation of model membrane systems on longer time and distance scales than are typically accessible at atomic resolution. Expansion of the spatial scale can be achieved through replication of the Markov transition matrix, to test whether oxygen diffusion over longer distances and multiple cell layers could be rate-limiting for oxygen delivery in some tissues. With the current bilayer systems, we have been able to reach simulation times of ~250 ns per hour, compared with 60–90 ns of MD simulation time per day on graphics processing unit (GPU) accelerators. The MCMC tech-

nique further enables modeling of intermittent variations, keeping in mind that RBCs are not continually at steady state.

The current results are intriguing, though further work is needed to determine their significance. The data indicate that membrane cholesterol diminishes the capacity of membranes to hold oxygen at steady state, with accompanying reduction in transmembrane oxygen flux. Additional study is required to evaluate whether hypercholesterolemia, and accompanying RBC membrane cholesterol elevation, would reduce RBC oxygen release to tissues. Such evaluation will require consideration of the effects of other potential barriers to oxygen diffusion. The structure of the vessel and target tissue presents many possible barriers, including the blood plasma, the endothelial cell membranes, and cytoplasm, as well as the interstitial fluid, membranes, and cytoplasm of the tissue. To a first approximation, the permeability of the aqueous layers immediately surrounding the RBC membrane should be considered: the RBC cytoplasm on one side and a layer of plasma on the other. Oxygen has relatively low solubility in water, compared with lipids, and is expected to have even lower solubility in aqueous fluids rich in proteins and other solutes [9, 10]. As such, the cytoplasm and plasma layers may pose diffusion barriers of comparable or greater magnitude than the RBC membrane barrier. Because permeability depends directly on thickness, close attention must be given to the thickness of the plasma layer surrounding the RBC. This layer may be especially thin in microcapillaries, where RBCs fit so snugly within the vessel that their shape is altered. In future work, we intend to pursue a formal comparison of the membrane barriers described here with aqueous barriers encountered upon O_2 transfer from RBCs to endothelial tissue.

References

1. Dotson RJ, Smith CR, Bueche K, Angles G, Pias SC (2017) Influence of cholesterol on the oxygen permeability of membranes: insight from atomistic simulations. Biophys J 112:2336–2347. https://doi.org/10.1016/j.bpj.2017.04.046. PMCID: PMC5474842

2. Widomska J, Raguz M, Subczynski WK (2007) Oxygen permeability of the lipid bilayer membrane made of calf lens lipids. Biochim Biophys Acta 1768:2635–2645. https://doi.org/10.1016/j.bbamem.2007.06.018. S0005-2736(07)00233-7 [pii]

3. Angles G, Dotson R, Bueche K, Pias SC (2017) Predicted decrease in membrane oxygen permeability with addition of cholesterol. Adv Exp Med Biol 977:9–14. https://doi.org/10.1007/978-3-319-55231-6_2. PMCID: PMC5673249

4. Durrett R (2012) Essentials of stochastic processes. Springer New York, New York, NY

5. Möller MN, Denicola A (2018) Diffusion of nitric oxide and oxygen in lipoproteins and membranes studied by pyrene fluorescence quenching. Free Radic Biol Med 128:137–143. https://doi.org/10.1016/j.freeradbiomed.2018.04.553

6. Python Software Foundation. The Python Language Reference, version 2.6.11. Available at http://www.python.org

7. Menchaca HJ, Michalek VN, Rohde TD, O'Dea TJ, Buchwald H (1998) Decreased blood oxygen diffusion in hypercholesterolemia. Surgery 124:692–698. https://doi.org/10.1067/msy.1998.90944. S0039-6060(98)00298-0 [pii]

8. Khan N, Shen J, Chang TY, Chang CC, Fung PC, Grinberg O, Demidenko E, Swartz H (2003) Plasma membrane cholesterol: a possible barrier to intracellular oxygen in normal and mutant CHO cells defective in cholesterol metabolism. Biochemistry 42:23–29. https://doi.org/10.1021/bi026039t

9. Battino R, Rettich TR, Tominaga T (1983) The solubility of oxygen and ozone in liquids. J Phys Chem Ref Data 12:163–178

10. Skulachev VP (1990) Power transmission along biological membranes. J Membr Biol 114:97–112